

Optimum shape to freeze hydrogels

Internship report

Noé Daniel *

ÉCOLE NORMALE SUPÉRIEURE

Under the supervision of **Lila Seguy, Suzie Protière and Axel Huerre.**

Internship done at Institut JEAN LE ROND D'ALEMBERT

June – July 2024



Département
de Physique
École normale
supérieure



Abstract

Les dynamiques de congélation de l'eau, connues sous le nom de problèmes de STEFAN, présentent des défis complexes, aussi bien théoriquement qu'expérimentalement. Ce stage se concentre sur un problème de STEFAN bidimensionnel en explorant la congélation d'hydrogels. Motivés par des similarités avec l'optimisation géométrique pour l'imbibition d'un capillaire par un fluide, notre but est de déterminer la géométrie optimale qui minimise le temps de congélation total d'un volume donné d'hydrogel. Au travers d'une analyse théorique et d'une vérification expérimentale, nous explorons différentes géométries pour aboutir aux congélations les plus rapides.

The freezing dynamics of water, known as STEFAN problems, present complex challenges in both theoretical and experimental contexts. This internship focuses on a two-dimensional STEFAN problem by exploring the freezing process of hydrogels. Motivated by similarities with shape optimization to reduce the wicking time in capillaries, our aim is to determine the optimal geometry that minimizes the total freezing time for a given volume of hydrogel. Through a combination of theoretical analysis and experimental validation, we explore various geometric configurations to find the fastest freezing time.

Keywords : Freezing, thermal diffusion, optimization

*. If you need to contact me : noe.daniel@ens.psl.eu

Acknowledgments

First and foremost, I would like to particularly thank my tutors : LILA SEGUY, SUZIE PROTIÈRE and AXEL HUERRE for supporting me throughout this internship and giving me a great introduction to experimental physics research. I would also like to thank P. VAN DE VELDE for allowing me to use his work as a basis for reflection and for his clarifications.

Beyond that, I would also like to thank the Institut Jean le Rond d'Alembert for hosting me and those I had the chance to meet in room 501 or in Salle Savart.

Table des matières

1 An Initial Experimental Approach	3
1.1 Description of the Experimental Setup	3
1.2 Creating the Hydrogel	4
1.3 What Does the Freezing Front Look Like?	4
2 Preliminary Experimental Observations	5
2.1 Influence of the Contact Surface with the Substrate	5
2.2 Towards Minimal Freezing Time?	5
2.3 Experimental Conclusions with Two Profile Types	6
2.4 Analysis of the Temporal Evolution of the Front	6
2.5 Slight Volume Expansion	7
3 Analytical Expressions for Freezing Times	8
3.1 General Expression for Freezing Time	8
3.2 What About the Different Profiles?	8
3.3 Limitations in Accessible Heights h_t ?	9
4 Comparison Between Theory and Experiment	10
4.1 The Results	10
4.2 What About the Exponential Profile?	10
4.3 Can We Conclude on an Optimal Shape? Power Laws.	10
4.3.1 Ratio $h_t/h < 1$	11
4.3.2 Ratio $h_t/h > 1$	11
4.3.3 What to Make of These Choices?	11
5 Annexe	14
5.1 Analyse d'image pour l'évolution du front	14
5.2 Expression du temps de congélation	15
5.3 Profil optimum avec le <i>Lagrangien</i>	15
5.4 Rapport h_t/h maximal accessible par z^α	16

Please note that this document is a translated version of my internship report that was originally written in French. Therefore some figures will still be labelled in French.

Introduction

In 2016, PIERRE VAN DE VELDE, formerly an intern at the University of Oxford, investigated optimal geometries to minimize the imbibition time of a fluid in capillaries, often referred to as *wicking time* [2, 8]. During this internship, we aim to undertake a somewhat similar approach by studying the optimal geometry that minimizes the freezing time of a hydrogel.

Freezing dynamics and phase change at the macroscopic scale have been current research topics for many years. While one-dimensional problems, such as the Stefan problem, have been extensively studied, two-dimensional or three-dimensional studies remain scarce.

Although the analogy between thermal and microfluidic processes seems quite intuitive, experimental approaches remain complex. Indeed, most attempts to solve freezing problems are mathematical or numerical rather than experimental.

1 An Initial Experimental Approach

1.1 Description of the Experimental Setup

We will study 3D axisymmetric hydrogels, so we restrict the study to a 2D analysis in the (r, z) plane with freezing along the z axis (FIG 2).

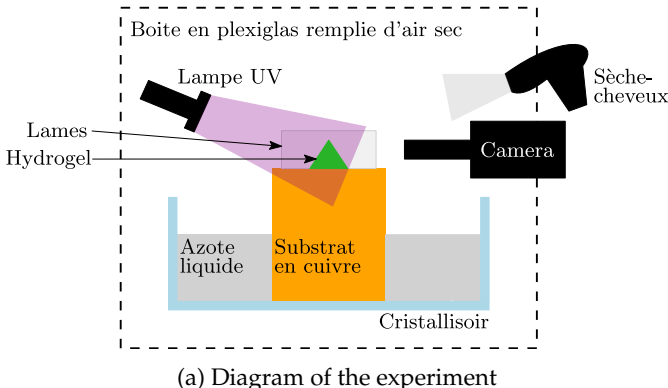
To achieve unidirectional freezing of our hydrogels, we use a copper substrate placed at a temperature below 0°C . Since we aim to reach temperatures below -100°C while conducting relatively short experiments, the substrate is placed in a crystallizer and cooled with liquid nitrogen (FIG. 1a).

To prevent humidity in the lab from causing frost on the substrate, the crystallizer and the copper cy-

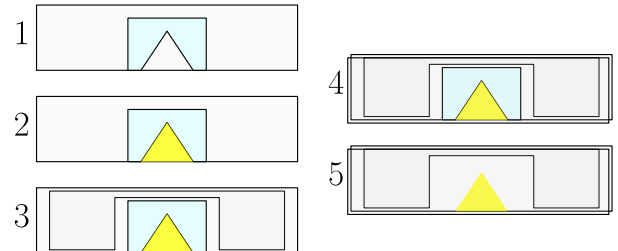
linder are placed inside a transparent acrylic box. We ensure there is an opening to allow the liquid nitrogen and dry air to enter, thereby removing moisture and reducing the risk of frost formation.

The hydrogels will be prepared with a 2% Agar concentration in fluorescent water. A custom-made acrylic support was designed using a laser cutter to ensure that the 2D hydrogels placed on microscope slides stand upright and maintain uniform contact with the substrate (FIG. 1a).

Moreover, the evolution of the ice front is moni-



(a) Diagram of the experiment



(b) Preparation of the hydrogel

FIGURE 1 – (a) 2D diagram of the experiment. Note that the substrate is connected to a thermocouple. The diagram is largely inspired by the one in [6]. (b) Steps for preparing the hydrogel once the solution is ready.

- 1) Place the silicone mold on a slide.
- 2) Add the still-liquid gel.
- 3) Place a small plastic piece called a "spacer" of the same thickness as the hydrogel and silicone to avoid damaging it during the next step.
- 4) Close with a second slide until solidification.
- 5) Remove the mold by taking off one slide, then replace the slide.

red via video analysis using a Nikon D800 camera with a 105mm, f 2.8 lens. Temperature readings are taken with a thermocouple placed at the substrate level. The gelled mixture does not fluoresce when in the solid (frozen) phase, thus allowing clear distinction of the water/ice boundary on video by adding UV light facing the hydrogel. Experimentally,

1.2 Creating the Hydrogel

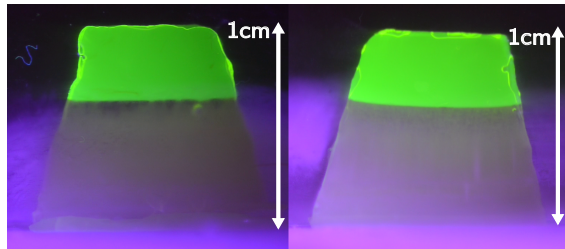
The study conducted by PIERRE VAN DE VELDE [8] showed that the exponential profile presented an optimum for inhibition time. Therefore, we will first study exponential and conical geometries (see TABLE 1, FIGURE 2) to try to validate or refute this conjecture.

Profile	$a(z)$
Rectangular	$a_0, \quad 0 \leq z \leq h$
Conical	$a_0(1 + \beta z), \quad 0 \leq z \leq h$
Quadratic	$a_0(1 + \mu z^2), \quad 0 \leq z \leq h$
Power α	$a_0 (1 + \mu_\alpha z^\alpha), \quad 0 \leq z \leq h$
Exponential	$a_0 \exp(\lambda z), \quad 0 \leq z \leq h$

TABLE 1 – Examples of different profiles

1.3 What Does the Freezing Front Look Like?

The STEFAN theory shows that in the 1D case, the front is perfectly horizontal [4]. Several studies indicate that outside the 1D case, the front is elliptical [5]. To simplify our study and the calculations related to the STEFAN condition, we desire a horizontal front.



(a) Observations for a truncated cone at $T = -80^\circ\text{C}$

only the still-liquid part of the hydrogel will fluoresce (FIG 3, 4).

Finally, to prevent fogging or frosting of the external surfaces of the acrylic, a hairdryer is placed above the camera to maintain good visibility throughout the experiment.

To create such hydrogels, we first make silicone molds with a thickness of $20\mu\text{m}$ using a plastic stencil or laser cutting. Once these molds are made, they are sandwiched between two microscope slides, and the gel, still liquid at $T \geq 70^\circ\text{C}$, is introduced. It gels as it cools, taking the shape of the mold (FIG 1B).

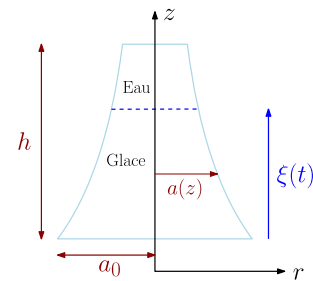
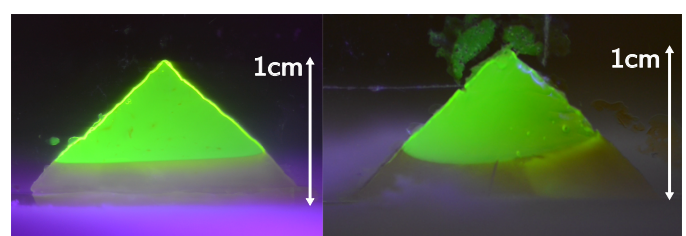


FIGURE 2 – Hydrogel described by its profile.

With a single slide, during the experiment, the front remains elliptical. However, by inserting the hydrogel between two microscope slides, the front becomes horizontal as shown in FIGURE 3. The thermal losses related to contact with the glass work in our favor to achieve such a front.



(b) Observations for a perfect cone at $T = -80^\circ\text{C}$

FIGURE 3 – The green fluorescent area is the still-liquid part of the hydrogel, while the transparent area is the frozen part of the hydrogel. For (a) and (b) : on the left : hydrogel between two slides; on the right : hydrogel on a single slide. For (a) and (b), the two photos correspond to two experiments with identical temperature and geometry conditions.

2 Preliminary Experimental Observations

The videos captured by the camera under UV light allow precise tracking of the freezing evolution by distinguishing the fluorescent area (liquid) from the transparent area (solid) (see FIGURE 4).

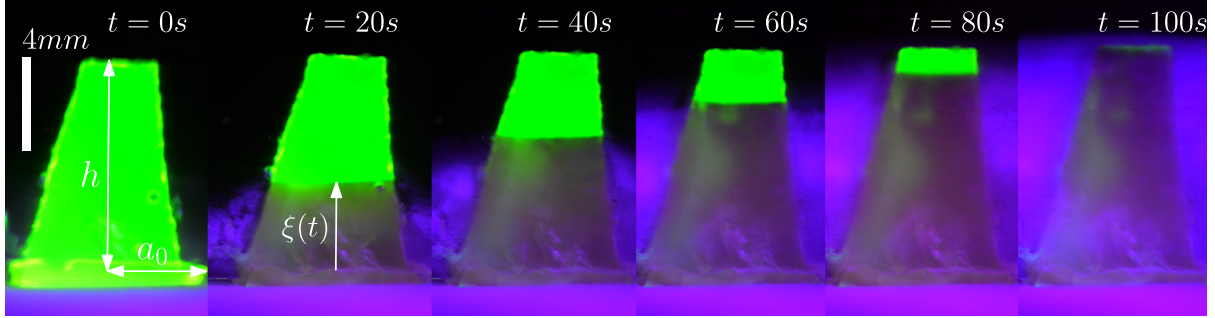


FIGURE 4 – 6 photographs at regular intervals during the freezing of a cone with height $h_t = 9.8$ mm.

2.1 Influence of the Contact Surface with the Substrate

We measure t_c , the total freezing time of a hydrogel, and considering conical hydrogels with the same area (equivalent to volume in 2D) of maximum height $h = 1\text{cm}$ but variable base radius a_0 (see FIGURE 2), we find that the contact surface (or line) a_0 plays a major role.

The lower the height of our hydrogel and the larger its contact surface with the substrate, the faster the freezing will occur (see FIGURE 5). The limiting case is to consider $h \rightarrow 0$ and $a_0 \rightarrow +\infty$ while keeping the hydrogel's volume constant.

2.2 Towards Minimal Freezing Time?

The goal of this stage is to find, for a fixed area and given contact surface with the substrate, the geometry that minimizes the freezing time denoted by t_c . These constraints can be expressed with equation (1).

$$A = \int_0^h a(z) dz \quad \text{and} \quad a(z=0) = a_0 \quad (1)$$

We compare freezing geometries to a rectangle of height h and base radius a_0 . It is observed that when the height of the hydrogel exceeds 1 cm or when the substrate temperature T_0 is below -50°C , the freezing times become abnormally long due to cryosuction. This phenomenon leads to a flux of water towards the freezing zone, increasing the amount to be solidified and prolonging the total freezing duration. Cryosuction can also induce porous structures, creating air pockets that thermally insulate certain parts of the hydrogel, slowing the propagation of freezing [9].

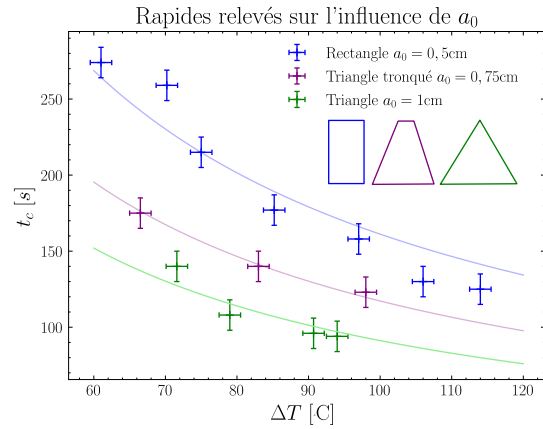


FIGURE 5 – Freezing time for different hydrogels with identical A and h but varying a_0 . Solid lines are fits in $1/\Delta T$. We will see in 3.1 that $t_c \sim 1/\Delta T$

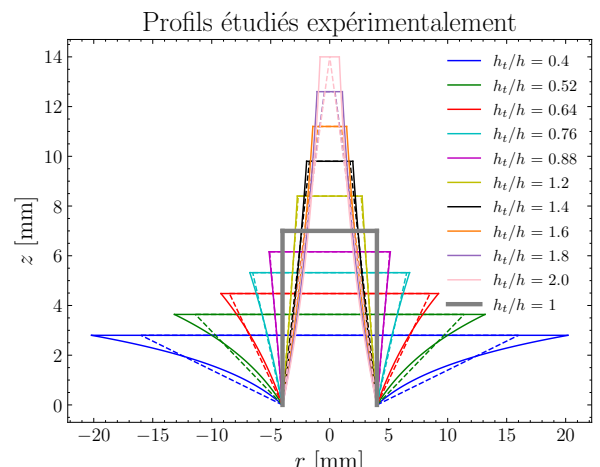


FIGURE 6 – Exponential and conical profiles, respectively, in solid and dashed lines. The reference rectangle is shown in thick gray.

To avoid these effects, we set a reference height of $h = 7\text{ mm}$ with $a_0 = 4\text{ mm}$ for our rectangle. The exponential and conical profiles studied have the

same area $A = a_0 h$ and the same contact surface a_0 , but different heights h_t . The study is conducted at $T_0 = -110^\circ\text{C}$ to ensure rapid freezing.

The constraints on the area, h_t , and a_0 uniquely determine each profile (TABLE 1, FIG 6). For the exponential profile, λ is obtained using equation (2), while β for the cone is determined by equation (3).

$$h = \frac{1}{\lambda} [\exp(\lambda h_t) - 1] \quad (2)$$

2.3 Experimental Conclusions with Two Profile Types

We again denote t_c as the final freezing time of the hydrogel as a function of the maximum gel height h_t . Experimental results (FIG 7) show that as h_t increases, t_c becomes larger. This is expected, but for a given height h_t , the conical hydrogel freezes faster than the exponential hydrogel across the entire range accessible to cones ($h_t \in [0, 2h]$).

Note that the behavior of the last points for heights $h_t \geq 1\text{cm}$ may be influenced by cryosuction.

$$h = h_t + \frac{\beta h_t^2}{2} \quad (3)$$

Only the exponential profile allows free choice of $h_t \in \mathbb{R}^{*+}$ due to its surjective nature and its ability to adjust to the reference area while increasing h_t . Other profiles, such as the cone, are limited ; for the cone, h_t must be within $[0, 2h]$. These limitations will be discussed in 4.3.

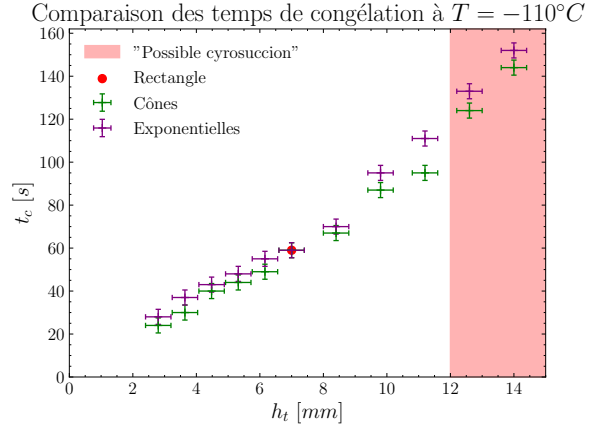


FIGURE 7 – Freezing times t_c as a function of the maximum height of the hydrogel h_t and its geometry for the substrate at $T = -110^\circ\text{C}$.

2.4 Analysis of the Temporal Evolution of the Front

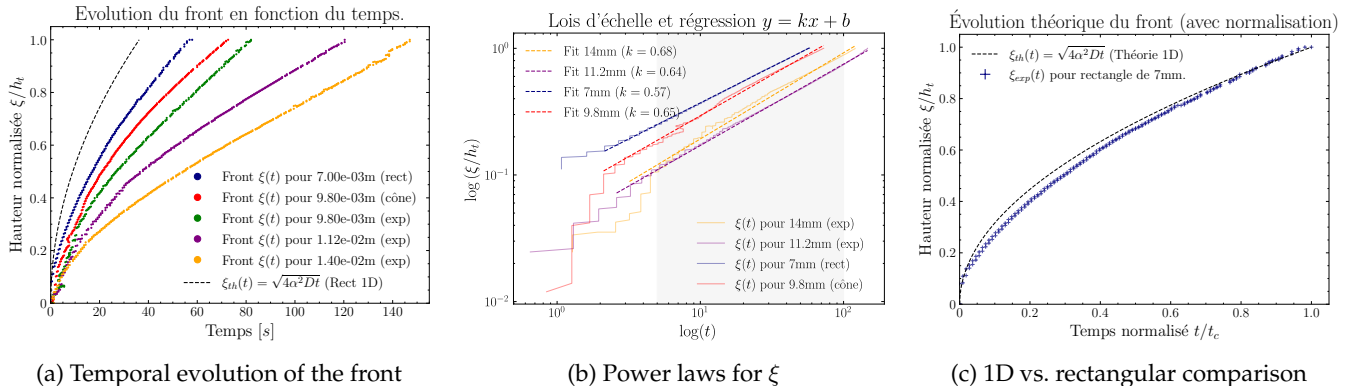


FIGURE 8 – Measurements performed with the substrate at $T = -110^\circ\text{C}$ (a) Evolution of the ice front for different hydrogels and the theoretical shape with the 1D STEFAN problem. Each evolution has been normalized by its maximum height h_t which varies according to the profiles. (b) Log-log space with several temporal evolutions of $\xi(t)$ to obtain the laws $\xi(t) \sim t^k$. (c) Shape of the front $\xi(t)$ in the 1D theoretical case and for a rectangle (2D) : the case closest to the 1D theory.

The freezing of the hydrogel is filmed at 30 frames per second. The videos converted into image sequences are then analyzed with *ImageJ*. The process is detailed in Appendix 5.1. This allows us to accurately access the curve $\xi = f(t)$ (FIG 8a).

The 1D STEFAN model predicts a front evolution of $\xi(t) \sim t^{1/2}$. Let's check if our profiles follow such

a power law (FIG 8b). The results are quite satisfactory with evolutions close to the square root of time, characteristic of a diffusive process.

In reality, the theoretical front evolution in the 1D case is more complex and is given by $h(t) = \sqrt{4\alpha^2 D_g t}$ where D_g is the diffusion coefficient of the solid phase and α is a solution of the transcenden-

tal equation (4) [6] where St is the Stefan number defined by : $St = \frac{c_{p,g}(T_F - T_0)}{L_{\text{fusion}}}$.

$$St = \sqrt{\pi} \alpha e^{\alpha^2} \operatorname{erf}(\alpha) \quad (4)$$

The shape of the front evolution between the 1D

theory and the rectangular profile is similar, with normalization (FIG 8c) : the theoretical freezing time is almost twice as short as the experimentally found one. However, the trend is extremely satisfactory.

2.5 Slight Volume Expansion

The density ratio of ice to water is about : $\frac{\rho_{\text{ice}}}{\rho_{\text{water}}} \simeq 0.93$. Thus, it is common to observe an increase of about 10% in volume when freezing a certain volume of water.

This phenomenon occurs during the freezing of the hydrogel and has been highlighted through videos. By calculating the number of pixels constituting the hydrogels before and after freezing, we obtain the percentage of volume expansion. The experiment shows an average of around 7-8%, which is consistent with what has been noted, notably in the work of L. SEGUY (*Thesis at d'Alembert*).

However, this value is not 9.3% since the hydrogel is not composed of 100% water but remains a polymer predominantly composed of water. Moreover,

the fluorescein added to the water to create a gel that shows up under UV light slightly modifies the density.

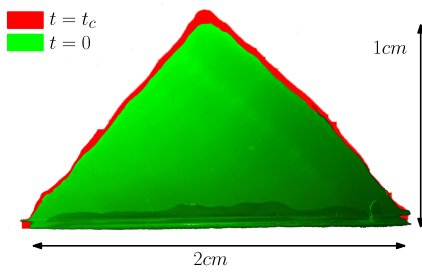


FIGURE 9 – Volume gained during freezing on two screenshots; the gained volume is shown in red.

3 Analytical Expressions for Freezing Times

3.1 General Expression for Freezing Time

As previously discussed, this problem is akin to reasoning already performed on capillaries [2, 8]. The FOURIER law is analogous to DARCY's law, and thermal flux to flow rate.

Consider a quasi-steady approach such that the linear thermal flux does not depend on z and is given by :

$$\varphi = a(z) \times \dot{\xi}(t) \quad (5)$$

The thermal current density in the aqueous phase is negligible compared to that in the solid phase, so FOURIER's law gives :

$$\frac{\varphi}{a(z)} = -\lambda_g \frac{\partial T}{\partial z} \quad (6)$$

The substrate is modeled as a thermostat with temperature T_0 , and at the interface at $z = \xi(t)$, the temperature is the freezing temperature of ice. Thus, $T(z = 0, r, t) = T_0$ and $T(z = \xi(t), r, t) = T_F = 0^\circ\text{C}$. We denote $T_F - T_0 = \Delta T$.

The condition at the water/ice interface (horizontal) is given by the STEFAN equation :

$$\rho_g L_{\text{fusion}} \dot{\xi}(t) = \lambda_g \left(\frac{\partial T}{\partial z} \right)_{\xi^-(t), r, t} - \lambda_l \left(\frac{\partial T}{\partial z} \right)_{\xi^+(t), r, t}$$

Using the STEFAN condition and FOURIER's law, we obtain the total freezing time t_c of the hydrogel given by equation (7). *Details of the calculation are provided in Appendix 5.2.*

$$Dt_c \equiv D_{\text{th}} \text{St } t_c = \int_0^h \left\{ a(\xi) \int_0^\xi a^{-1}(z) dz \right\} d\xi \quad (7)$$

Where $D_{\text{th}} = \frac{\lambda_g}{\rho_g c_{p,g}}$ is the classical thermal diffusion coefficient and $\text{St} = \frac{c_{p,g} \Delta T}{L_{\text{fusion}}}$ is the Stefan number. Thus, we find a diffusive problem similar to the case of capillaries. [2, 8]

We see that for a fixed profile, t_c evolves as $1/\Delta T$. We perform measurements at different T for the

3.2 What About the Different Profiles ?

We return to the experimental approach where our reference profile is a rectangle with half-width a_0 and height h . All profiles thus have the same area : $A = a_0 h$. Using formula 7, we can analytically determine the freezing times for different profiles.

The exponential profile has a freezing time given by (8), the conical profile by (9), and the quadratic profile by (10). *Parameters λ, β, μ are listed in TABLE 1.*

same rectangular profile to verify this result (FIG 10) and the agreement is satisfactory.

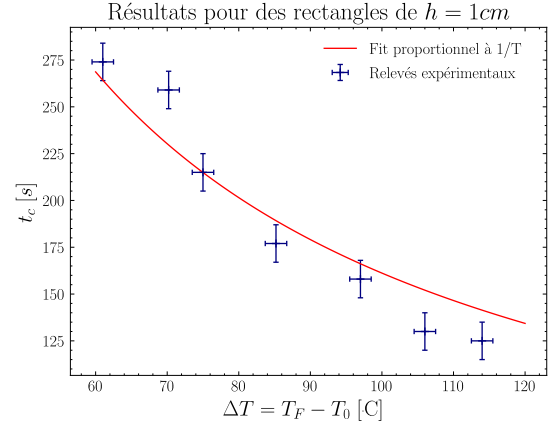


FIGURE 10 – Evolution of freezing times for the same profile ($h = 1\text{cm}$, $a_0 = 5\text{m}$) at different substrate temperatures.

It is also noteworthy that when considering a constant profile of the form $a(z) = a_0$, we obtain : $Dt_c = \frac{h^2}{2}$. Thus, the ice penetration height grows as $h \sim t^{1/2}$. This demonstrates the thermal analogue of the BELL-CAMERON-LUCAS-WASHBURN (BCLW) law for capillaries, which states that the penetration length L of a fluid into a capillary evolves as $L \sim t^{1/2}$ [2, 3, 8].

Can We Find an Optimum ?

As mentioned at the beginning of our study, the goal is to find a profile $a(z)$ that minimizes the final freezing time t_c for a fixed area and identical substrate contact, i.e., the same contact surface area. The constraint was already formulated with (1).

By performing a Lagrangian optimization (*details in appendix 5.2*), the optimal solution should be of the form : $a(z) = a_0 \exp(\lambda z)$, as found by P. VAN DE VELDE [8].

It is particularly interesting that the freezing time for such profiles does not depend on the contact surface area a_0 . This highlights that there is effectively only one control parameter, which is the height of the hydrogel.

Finally, few cases $a(z)$ have analytical solutions. Only the profiles z , z^2 , and \exp will be studied analytically. For the others, numerical integration is used.

$$Dt_{c,exp} = -\frac{h_t}{\lambda} + \frac{1}{\lambda^2}[\exp(\lambda h_t) - 1] \quad (8)$$

$$Dt_{c,cone} = \frac{1}{2\beta^2} (1 + \beta h_t)^2 \ln(1 + \beta h_t) - \frac{1}{4\beta^2}[(1 + \beta h_t) - 1] \quad (9)$$

$$Dt_{c,quad} = \frac{-\mu h_t^2 - 2 \log(1 + \mu h_t^2) + 2\sqrt{\mu} h_t (\mu h_t^2 + 3) \arctan(\sqrt{\mu} h_t)}{6\mu} \quad (10)$$

3.3 Limitations in Accessible Heights h_t ?

As briefly mentioned earlier, conical profiles only allow for heights h_t such that $h_t \in]0, 2h]$. Subsequently, we will use normalized heights h_t/h . This limitation is not unique to cones; it exists for all power laws z^α with a maximum accessible ratio h_t/h denoted $\Theta_\alpha \equiv h_{t\alpha}/h$.

This maximum value $h_{t\alpha}$ corresponds to the first root of the profile $a(z) = a_0(1 + \mu_\alpha z^\alpha)$. Otherwise, for $h_t > h_{t\alpha}$, the left and right edges overlap. Using

the calculations from 3.1, we determine Θ_α precisely. The quick calculations are left in appendix 5.4. We find :

$$\Theta_\alpha = \frac{\alpha + 1}{\alpha} \geq 1 \quad (11)$$

Thus, regardless of the chosen law z^α , one can always create a hydrogel with this profile for heights $h_t \leq h$ i.e., $(h_t/h \leq 1)$ (i.e., increasing profiles). These limitations are important for the experimenter, who cannot freely choose the ratio h_t/h .

4 Comparison Between Theory and Experiment

4.1 The Results

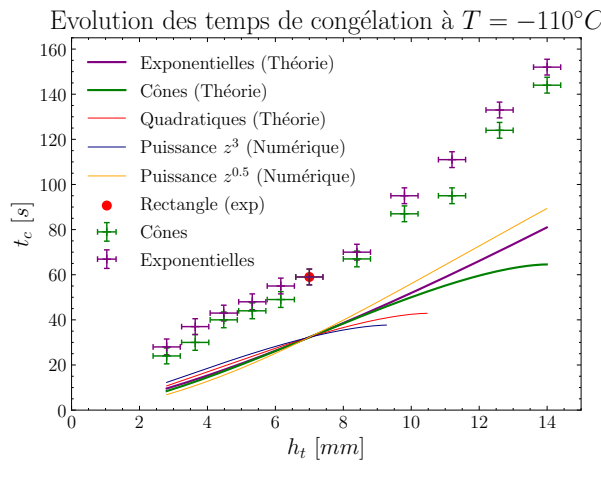
With the expressions for freezing times (9, 8), we can obtain the behavior of $t_{c,\text{cone}}$ and $t_{c,\text{exp}}$ as a function of h_t . This is represented in Figure 11a. The theory aligns with the experiment and predicts a faster freezing time for cones compared to exponentials.

The discrepancy between theoretical and experimental values (FIG 11a) is non-negligible and can be explained by losses due to plates, the assumption of a perfect thermostat for the substrate, or the constant flux. However, when normalized, the

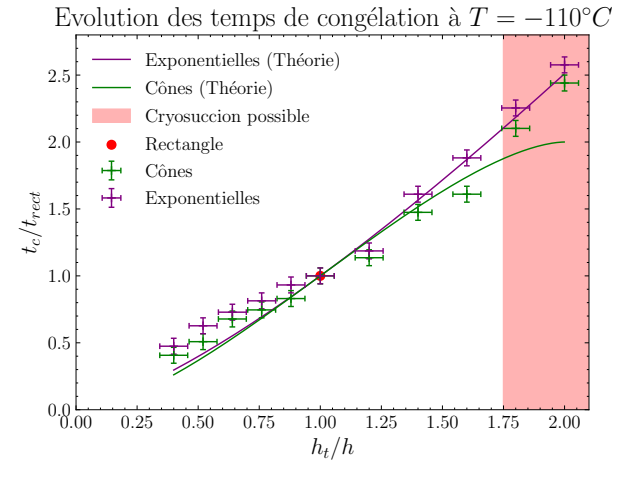
trend remains very convincing as seen in Figure 11b.

The agreement between theory and experiment confirms the relevance of our model, which will allow us to explore other profiles later.

The results may seem surprising since the constrained optimization suggested that the exponential profile was optimal. However, by examining profiles in z^α (FIG 11a), we find that it is possible to achieve both faster and longer freezing times than the exponential.



(a) Without normalization



(b) Theory and experiment

FIGURE 11 – (a) Evolution of t_c as a function of h_t and the profiles. The discrepancy between theory and experiment is noticeable (27s difference for the rectangle, for example). (b) Normalized freezing times as a function of normalized profile heights. For experimental values, normalization in the ordinate is done with respect to the freezing time of the rectangle obtained during experiments (≈ 59 s). For theoretical values, normalization is done with respect to the theoretical freezing time of the rectangle (≈ 32 s).

4.2 What About the Exponential Profile?

The exponential profile cannot be a global minimum or maximum since families of profiles contradict this result. Why does this profile appear at the end of the constrained optimization?

Firstly, the exponential profile might simply be a local optimum within the family of profiles. We might have explored several profiles not close to exponential profiles in the profile space.

In another measure, this could be related to the sur-

jective nature of the function $\exp : \mathbb{R}^+ \rightarrow \mathbb{R}^{+*}$. Indeed, if z^α profiles are constrained by the accessible ratios h_t/h Section (3.3), the exponential profile can adjust its curvature very strongly, allowing it to satisfy any area constraint at any maximum height h_t .

Thus, it is reasonable to think that the optimization returns this profile to ensure “at least” the existence of a profile that satisfies the constraints for any values of h and h_t .

4.3 Can We Conclude on an Optimal Shape? Power Laws.

We chose to study only a specific range of profiles during this stage, namely : exponential, conical, rectangular, and power laws. As observed in 4.1, to mi-

nimize t_c as much as possible, one should consider the smallest possible ratio h_t/h .

What if the experimenter is limited in their choice

of h_t/h or desires a given height h_t ?

4.3.1 Ratio $h_t/h < 1$

If the experimenter wishes to design the hydrogel (*respecting (1)*) with height h_t and $h_t/h < 1$, **the observations show that they should choose a power law profile z^α with $\alpha < 1$ and α as small as possible.** (FIG 12a, b)

Figure 12b also shows that only power laws z^α with $\alpha \geq 1$ have a freezing time lower than that of the exponential profile over the entire range $h_t/h \in]0, 1]$.

4.3.2 Ratio $h_t/h > 1$

If the experimenter wishes to design a hydrogel with height h_t such that $h_t/h > 1$, **they will often**

need to choose a power law.

Observations from Figure 12c indicate that for a chosen ratio h_t/h , the profile that seems to minimize the freezing time would be the power law α such that $\Theta_\alpha = h_t/h$. Knowing the expression relating Θ_α to α , we obtain the optimal power for a ratio $h_t/h > 1$. We can then plot the minimal freezing time t_c obtained with the optimal power at each value of h_t/h (FIG 12d).

Zooming in on Figure 12c highlights that only powers $\alpha \geq 1$ are better than the exponential over their entire range $h_t/h \in [1, \Theta_\alpha]$. However, for any $\alpha \geq 1$, $\Theta_\alpha \leq 2 = \Theta_1$.

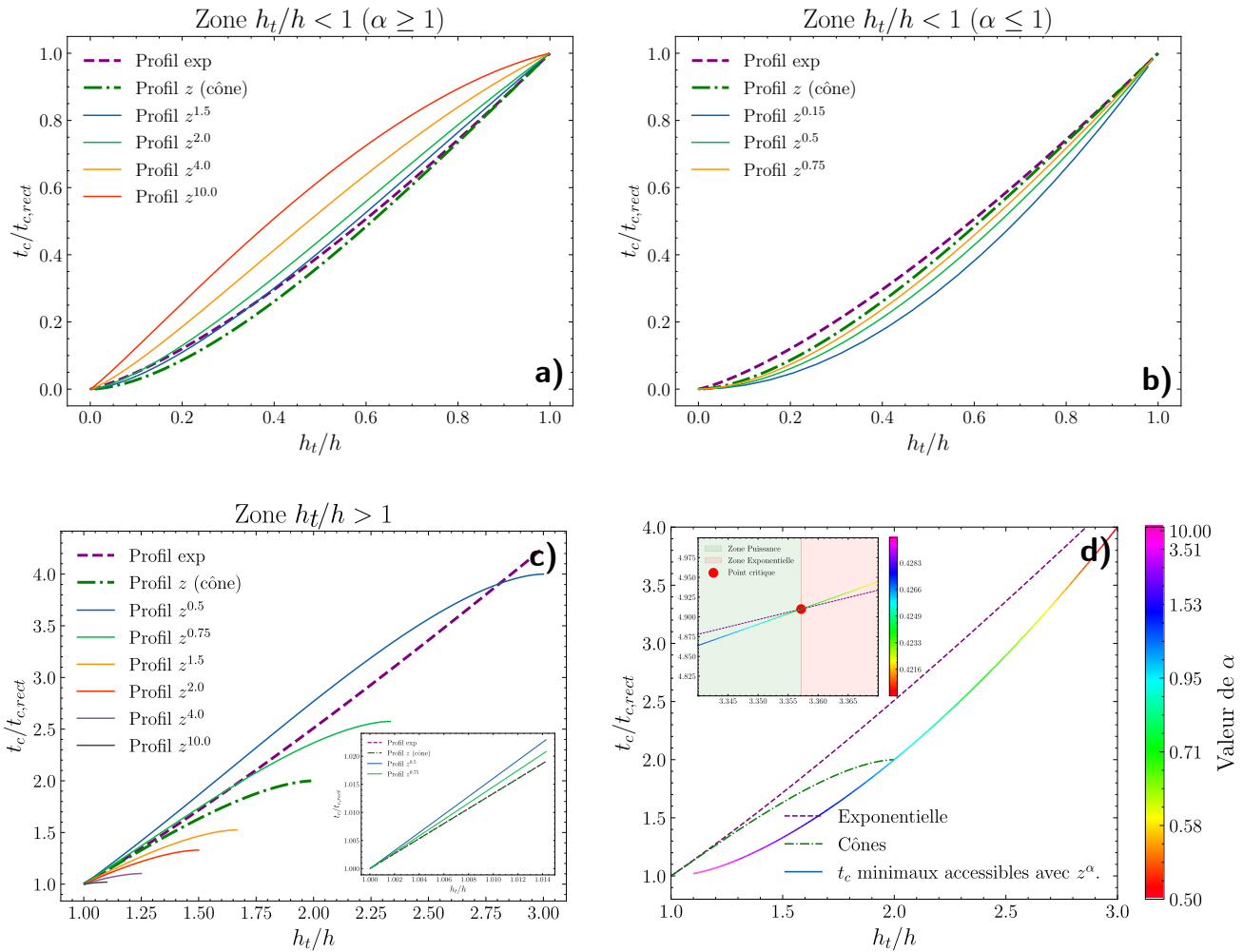


FIGURE 12 – (a) and (b) Graphs showing $t_c/t_{c,rect} = f(h_t/h)$ for power law profiles z^α with solid lines. Note that these curves are identical regardless of the values of h or T_0 . (c) Highlighting a **possible** optimal solution : power law. (d) Visualization of minimal times accessible by power laws compared to exponentials. Highlighting two zones where power laws and exponentials are the best choices, respectively. The RGB curve is not extended to $(1,1)$ as it corresponds to values of $\alpha \in [10, +\infty[$.

4.3.3 What to Make of These Choices ?

In light of our results, among regular continuous profiles (\exp, z^α, \dots), power laws provide the best freezing times for $h_t/h \leq \Theta_{lim} \simeq 3.3557$. Their only "drawback" is the variable range of accessible ratios h_t/h when considering such ratios greater than 1.

By applying the approach outlined above according to the chosen value of h_t , one ensures minimal freezing time. Of course, if the contact surface area with the thermostat is not restricted, the optimal strategy is to maximize a_0 and minimize h . Note, however, that **height is the crucial parameter since it is not very realistic to achieve $a_0 \rightarrow \infty$** .

Conclusion

This study highlights the relevant parameters to consider when choosing the shape of a hydrogel to freeze as quickly as possible in a unidirectional manner. Indeed, height and contact surface play a crucial role in optimization.

While cylindrical geometry might seem like the intuitive choice, we conclude that conical and exponential shapes, which initially appeared to be the most suitable competitors, result in very different freezing times. Ultimately, for fixed contact and volume, power laws are the best candidates for reducing freezing times for low ratios h_t/h , and exponential profiles are preferable for higher h_t/h ratios.

Références

- [1] D. Caccavo, S. Cascone, G. Lamberti, and A. A. Barba. Hydrogels : experimental characterization and mathematical modelling of their mechanical and diffusive behaviour. *Chemical Society Reviews*, 47(7) :2357–2373, 2018.
- [2] E. Elizalde, R. Urteaga, and C. L. A. Berli. Rational design of capillary-driven flows for paper-based microfluidics. *Lab on a Chip*, 15(10) :2173–2180, 2015.
- [3] J.-B. Gorce, I. J. Hewitt, and D. Vella. Capillary imbibition into converging tubes : Beating washburn’s law and the optimal imbibition of liquids. *Langmuir*, 32(6) :1560–1567, feb 2016.
- [4] A. H. Harker. The classical stefan problem : basic concepts, modelling and analysis with quasi-analytical solutions and methods. *Contemporary Physics*, 59(4) :428–429, oct 2018.
- [5] N. Ohara, B. M. Jones, A. D. Parsekian, K. M. Hinkel, K. Yamatani, M. Kanevskiy, R. C. Rangel, A. L. Breen, and H. Bergstedt. A new stefan equation to characterize the evolution of thermokarst lake and talik geometry. *The Cryosphere*, 16(4) :1247–1264, apr 2022.
- [6] L. Seguy, S. Protiere, and A. Huerre. Role of geometry and adhesion in droplet freezing dynamics. *Physical Review Fluids*, 8(3) :033601, mar 2023.
- [7] M. Stiti, G. Castanet, A. Labergue, and F. Lemoine. Icing of a droplet deposited onto a subcooled surface. *International Journal of Heat and Mass Transfer*, 159 :120116, oct 2020.
- [8] P. Van de Velde. Internship report, paper microfluidics, 2016.
- [9] M. G. Worster, S. Peppin, and J. Wettlaufer. Colloidal mushy layers. *Journal of Fluid Mechanics*, 914 :A28, May 2021.

5 Appendix

5.1 Image Analysis for Front Evolution



FIGURE 13 – Steps for image analysis

Experiments are largely analyzed using the obtained video file. It is possible to sequence it to create images every 0.5s of this video. This is called sequencing.

Then, the software *ImageJ* allows for the analysis of these image sequences. The goal is to track the evolution of the front along a line that goes perpendicularly from the top to the bottom of the hydrogel (*add figure*).

With the *Reslice* option, we can observe the evolution of the pixels along this line across all images (i.e., as a function of time with a step of 0.5s).

By separating the color *channels* and taking the green *channel* and applying a treatment to convert the image to binary (black and white), we obtain a usable reslice.

Indeed, using Python's OpenCV library, we can outline the areas of the same color and thus obtain the curve marking the boundary between the black and white areas, which is $\xi = f(t)$. This is how we obtain the curves in FIGURE 8a.

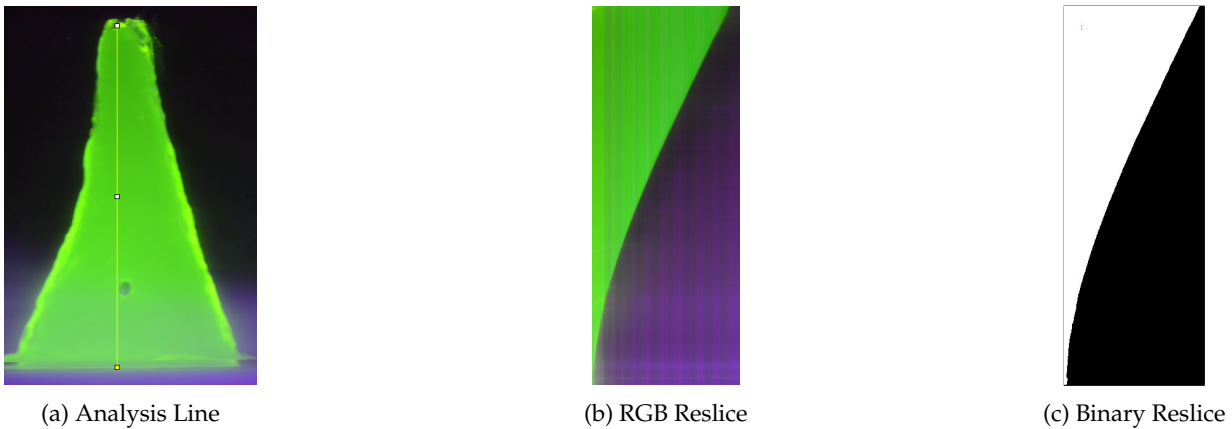


FIGURE 14 – (a) Creation of the analysis line on which the reslice will be performed. *It is shown in yellow in the screenshot.* (b) Obtained reslice. Each vertical column of 1 pixel corresponds to the yellow line. These columns are overlaid from left to right over the image sequence. (c) Processed reslice transformed into binary to obtain the profile $\xi = f(t)$ which is the boundary between the white and black areas.

By knowing the scale between px and time s , we can obtain the curve in FIGURE 15 after Python outlining.

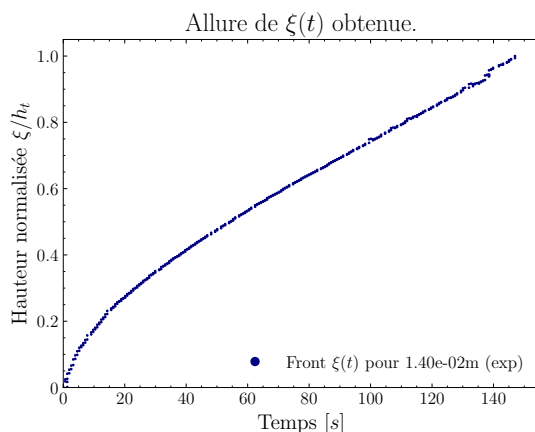


FIGURE 15 – Result of the processing via ImageJ + OpenCV

5.2 Expression of Freezing Time

Consider an axisymmetric profile with half-length $a(z)$ and height h . The ice front is denoted by $\xi(t) \in [0, h]$.

A quasi-stationary approach is considered so that φ (linear thermal flux) does not depend on z :

$$\varphi = a(z) \times \dot{\xi}(t) \quad (12)$$

The thermal current density in the aqueous phase being negligible compared to that in the solid phase, Fourier's law gives :

$$\frac{\varphi}{a(z)} = -\lambda_g \frac{\partial T}{\partial z} \quad (13)$$

The substrate acts as a perfect thermostat and we consider $T(z = 0, r, t) = T_0$ and $T(z = \xi(t), r, t) = T_F$. Let $T_F - T_0 = \Delta T$

By separating variables, we obtain :

$$\int_0^\xi a^{-1}(z) dz = -\frac{\lambda_g(T_F - T_0)}{\varphi} = \frac{-\lambda_g \Delta T}{\varphi} \quad (14)$$

The condition at the interface between the water and ice is obtained by an enthalpy and mass balance which leads to the Stefan equation :

$$\rho_g L_{\text{fusion}} \dot{\xi}(t) = \lambda_g \left(\frac{\partial T}{\partial z} \right)_{\xi^-(t), r, t} - \lambda_l \left(\frac{\partial T}{\partial z} \right)_{\xi^+(t), r, t}$$

Neglecting the thermal density of water, we get :

$$\rho_g L_{\text{fusion}} \dot{\xi}(t) = \lambda_g \left(\frac{\partial T}{\partial z} \right)_{\xi^-(t), r, t} = -\frac{\varphi}{a(\xi)} \quad (15)$$

A second separation of variables yields :

$$\frac{a(\xi) d\xi}{\varphi} = -\frac{dt}{\rho_g L_{\text{fusion}}}$$

By combining the previous equation, we obtain :

$$\frac{\lambda_g \Delta T}{\rho_g L_{\text{fusion}}} dt = \left\{ a(\xi) \int_0^\xi a^{-1}(z) dz \right\} d\xi$$

Thus, the total freezing time t_c of the hydrogel is given by the equation (16) :

$$Dt_c \equiv D_{\text{th}} \text{St } t_c = \int_0^h \left\{ a(\xi) \int_0^\xi a^{-1}(z) dz \right\} d\xi \quad (16)$$

With $D_{\text{th}} = \frac{\lambda_g}{\rho_g c_{p,g}}$ the classical thermal diffusion coefficient and $\text{St} = \frac{c_{p,g} \Delta T}{L_{\text{fusion}}}$ the Stefan number.

5.3 Optimal Profile with the Lagrangian

With the constraint (1), the action to consider is :

$$\int_0^h \left(a(\xi) \int_0^\xi a^{-1}(z) dz \right) - \lambda \int_0^h a(\xi) d\xi = \int_0^h a(\xi) \left(\int_0^\xi a^{-1}(z) dz - \lambda \right) d\xi$$

First, let $I(z) = \int_0^z a^{-1}(y) dy$ and note that $a(z) = 1/I'(z)$. Now introduce the Lagrangian of the problem :

$$\mathcal{L} = \frac{I(z) - \lambda}{I'(z)}$$

The Euler-Lagrange equations yield :

$$\frac{d\mathcal{L}}{dz} = \frac{d}{dz} \left(\frac{I(z) - \lambda}{I'(z)} \right) = 0 \quad (17)$$

Since $I(z=0) = 0$ and $a(z=0) = a_0 = \frac{1}{I'(z=0)}$, we get :

$$\frac{dI}{dz} + \frac{I}{\lambda a_0} = \frac{1}{a_0} \quad (18)$$

Which leads to an exponential solution for $a(z)$ of the form :

$$a(z) = a_0 \exp \left(\frac{z}{\lambda a_0} \right)$$

By redefining λ if necessary, these profiles will subsequently be simply given by : $a(z) = a_0 \exp(\lambda z)$.

5.4 Maximum h_t/h Ratio Accessible by z^α

In this subsection, we want to analytically find the expression for the maximum h_t/h ratio that a hydrogel can achieve with a power law α . That is, with a profile : $a(z) = a_0(1 + \mu_\alpha z^\alpha)$. This limit value has been introduced in the report with the notation $\Theta_\alpha = h_{t\alpha}/h$.

This maximum value $h_{t\alpha}$ actually corresponds to the first root of the profile $a(z) = a_0(1 + \mu_\alpha z^\alpha)$. Otherwise, for $h_t > h_{t\alpha}$, the profile intertwines.

Initially, we know that $a(h_{t\alpha}) = a_0(1 + \mu_\alpha h_{t\alpha}^\alpha) = 0$. This imposes the choice of μ_α with : $\mu_\alpha = -h_{t\alpha}^\alpha$

The area conservation (1) imposes a condition on μ_α :

$$h = h_{t\alpha} + \mu_\alpha \frac{h_{t\alpha}^{\alpha+1}}{\alpha + 1} \quad (19)$$

Substituting μ_α , we obtain :

$$\Theta_\alpha = \frac{\alpha + 1}{\alpha} \geq 1 \quad (20)$$